Brønsted acid-catalyzed tert-butylation of phenol, *o*-cresol and catechol: A comparative computational study

Xiaowa Nie [a,b], Xin Liu [a], Chunshan Song [a,b,*], Xinwen Guo [a,**]

[a] *State Key Laboratory of Fine Chemicals, Department of Catalysis Chemistry and Engineering, School of Chemical Engineering, Dalian University of Technology, Dalian 116012, PR China*
[b] *EMS Energy Institute and Department of Energy & Mineral Engineering, Pennsylvania State University, University Park, PA 16802, USA*

ABSTRACT

SO$_3$H-functionalized ionic liquids (FILs) have been used to catalyze the alkylation of phenol, *o*-cresol and catechol with tert-butyl alcohol (TBA), and the catalytic performances are promising. During these Brønsted acid-catalyzed tert-butylations, *t*-butyl phenol ether (TBPE) and *t*-butyl *o*-cresol ether (TBOCE) are found, but no *t*-butyl catechol ether (TBCE) is detected. With the help of density functional theory (DFT) calculations, the reaction mechanisms of Brønsted acid-catalyzed tert-butylation of phenol, *o*-cresol and catechol were examined. The steric effect of *t*-butyl group does not have an apparent impact on the regioselectivity to *t*-butyl ether. The differences in the stability of O-alkylation intermediates, resulted from different ortho-substituents, account for the regioselectivity to *t*-butyl ether. For catechol tert-butylation, an intramolecular hydrogen bond is formed within the O-alkylation intermediate, which leads to extra stability of this intermediate and obvious increase of the activation barrier for TBCE formation. The intramolecular hydrogen bond formed within the O-alkylation intermediate facilitates its isomerization, inhibits the TBCE formation, thus making the reaction kinetics for catechol tert-butylation unique.

© 2010 Elsevier B.V. All rights reserved.

1. Introduction

Ionic liquids (ILs) have been applied and found to be effective in some catalytic conversions [1–4]. Apart from their superior catalytic performances, they also exhibit unique characteristics, such as low vapor pressure, excellent chemical and thermal stability, recoverability and convenience in product separation [5–8]. Especially, the Brønsted acidic functionalized ionic liquids (FILs) have been reported as novel eco-benign catalysts for some acid catalyzed reactions [9–12].

Our laboratory-synthesized SO$_3$H-functionalized ionic liquids (SO$_3$H-FILs) show promising catalytic performances on tert-butylation of phenol, *o*-cresol and catechol with tert-butyl alcohol (TBA) [13–17], and the results on conversion and selectivity as a function of reaction time are illustrated in Supporting Information Fig. S1. Under the optimum reaction conditions with the most promising [(CH$_3$)$_3$N(CH$_2$)$_4$SO$_3$H][HSO$_4$] ionic liquid, tert-butylation of phenol yielded a conversion of phenol as high as 79.6% and selectivity to 2-tert-butyl phenol (2-TBP) as 52.4% [13].

The conversion of *o*-cresol was 80.9%, and the selectivity to 4-tert-butyl *o*-cresol (4-TBOC) was 44.1%. The conversion of catechol and the selectivity to 4-tert-butyl catechol (4-TBC) could reach 41.5% and 97.1%, respectively [14]. In experiments, the selectivity to *t*-butyl phenol ether (TBPE) can reach nearly 35% and is almost the same as that to 2-tert-butyl phenol (2-TBP) at the beginning of phenol tert-butylation. As the reaction time goes, the selectivity to C-alkylation products increases at the expense of TBPE selectivity [13]. The reaction kinetics for *o*-cresol tert-butylation is similar to that for phenol, however, the reaction properties for catechol tert-butylation are dramatically different from those for phenol and *o*-cresol [14,15]: the products are mixture of only C-alkylation products, and *t*-butyl catechol ether (TBCE) is not detected throughout the reaction, which is in agreement with the previous studies by Yoo et al. [18] and Zhou et al. [19]. Experimental results indicate a strong dependence of the reaction path on the nature and structure of the reactant, but little is known on the detailed conversion mechanisms of these Brønsted acid-catalyzed tert-butylations and the factors impacting the selectivity to *t*-butyl ether.

In this work, with the help of density functional theory (DFT) calculations, we examined the reaction mechanisms of Brønsted acid-catalyzed tert-butylation of phenol, *o*-cresol and catechol, and explained the regioselectivity to *t*-butyl ether at a molecular level. Instead of the steric effect due to the size and structure of *t*-butyl agent and the ortho-substituent within the reactant molecule, we found that the intramolecular hydrogen bond formed

* Corresponding author. Tel.: +1 814 863 4466; fax: +1 814 865 3573.
** Corresponding author at: Dalian University of Technology, PO Box 39, No. 158 Zhongshan Road, Dalian 116012, PR China. Tel.: +86 411 39893990; fax: +86 411 39893991.
E-mail addresses: csong@psu.edu (C. Song), guoxw@dlut.edu.cn (X. Guo).

Table 1
Parameters for PCM salvation-model used in phenol, o-cresol and catechol tert-butylation.

Parameter	Solvent	Eps	RSolv	NSphG
Phenol tert-butylation	Cyclohexane	2.023	2.815	18
o-Cresol tert-butylation	Cyclohexane	2.023	2.815	18
Catechol tert-butylation	Toluene	2.379	2.820	19

within O-alkylation intermediate has a significant impact on the regioselectivity to TBCE, and alter the reaction kinetics of catechol tert-butylation.

2. Computational methods

The current work aims at examining the reaction mechanisms and uncovering the factors impacting the regioselectivity to t-butyl ether in phenol, o-cresol and catechol tert-butylations. As these reactions are Brønsted acid catalyzed conversions, proton transfer among the components should be vital. The molecular structures of the experimentally synthesized SO_3H-FILs (IL1–IL4) [13–15] are provided in Supporting Information Table S1. The cation group (quaternary ammonium part) of SO_3H-FIL plays a minor role in catalyzing these reactions [13–17], so a simple Brønsted acid model can be adopted to represent the SO_3H-FIL. A CH_3SO_3H molecule includes a sulfonic group, and its acid site strength is similar to that of quaternary ammonium ion substituted sulfonic acid FILs (IL1–IL4) according to the DFT calculation results on proton affinities (PAs) of these Brønsted acid models (PA for CH_3SO_3H is −1349.0 kJ/mol, while it is −1312.7, −1344.9, −1325.1 and −1357.8 kJ/mol for IL1, IL2, IL3 and IL4, respectively). To balance the need for setting up a representative model and the computational efficiency, a CH_3SO_3H was introduced to represent the SO_3H-FIL as a Brønsted acid catalyst.

All the calculations were performed using Gaussian 03 package [20]. The equilibrium geometries were obtained by Becke-style three-parameter functional (B3) with the Lee–Yang–Parr correlation functional (LYP) within the framework of DFT at the 6-311 + G(d,p) level [21–24]. The stability of the wave function was tested for each state, and zero point energy (ZPE) corrections were included. Local atomic charge and frontier electron density [$f_r(E)$] were calculated. Transition states were located using the QST [19] method in DFT. Each transition state was confirmed by the single imaginary frequency along the reaction coordinate first, and then by the intrinsic reaction coordinate (IRC) scan [25,26].

The polarized continuum model (PCM) developed by Tomasi [27–30] was employed to include the impact of solvent. In this model, the atomic radii of the sphere used to build the molecular cavity was adjusted by involving consideration of local chemical environment, such as hybridization, formal charge, and first neighbor inductive effect. The impact of the escaped electronic charge outside the cavity was corrected with an additional set of charge on the cavity surface distributed according to the solute electronic density in each point of the surface. In this study, we introduced cyclohexane solvent for phenol and o-cresol tert-butylation, and toluene solvent for catechol tert-butylation based on the experimental work [13,14]. The parameters employed in PCM are given in Table 1.
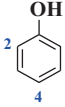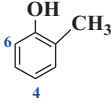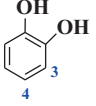
3. Results and discussion

In our recent work [15], we proposed two reaction paths for catechol tert-butylation with t-C_4H_9OH, one mechanism with t-C_4H_9OH as the t-butylation agent directly without dehydration, and the other mechanism with dehydration of t-C_4H_9OH by interaction with CH_3SO_3H to produce the CH_3SO_3–t-C_4H_9 (sulfonic ester inter-

mediate, as proposed also in Tang's work [31]) as the t-butylation agent. We compared the kinetic differences between these two proposed mechanisms, and found that the mechanism with t-C_4H_9OH as the direct t-butylation agent is kinetically more favored than that with CH_3SO_3–t-C_4H_9 as the t-butylation agent in terms of the activation barrier (E_a), thus determined the acid-assisted SN2 process without t-C_4H_9OH dehydration as the main reaction route for catechol tert-butylation. The reaction paths for phenol, o-cresol and catechol tert-butylation should be similar, thus in this work, we discussed the favored acid-assisted SN2 mechanism without TBA dehydration for Brønsted acid-catalyzed tert-butylation of phenol, o-cresol and catechol as: the initial reaction mixture is composed by Brønsted acid catalyst (CH_3SO_3H), phenol reactant, TBA, and organic solvent such as cyclohexane or toluene. TBA attacks phenol, o-cresol or catechol with CH_3SO_3H-assisted interaction to produce the mono-C-alkylation or O-alkylation intermediate, releasing a water molecule. Then the formed negatively charged $CH_3SO_3^-$ anion transfers to interact with the proton of the protonated intermediate to form the second alkylation intermediate. Through deprotonation of the second alkylation intermediate, the C-alkylation product or t-butyl ether is produced. t-Butyl ether formation is reversible, and the O-intermediate can isomerize to produce the C-intermediates in this acidic mixture. Partial mono-C-alkylation product is further alkylated to produce the di-alkylation product with the reaction proceeding. Among the reaction species, only the hydroxyl groups of phenol, o-cresol or catechol, the –SO_3H group within CH_3SO_3H and the protonated intermediates exhibit reasonable proton affinities [13–15]. The organic solvents employed are cyclohexane or toluene, thus the proton transfer, inside the dilute organic solution with a lower solvent proton affinity, is only included in those O-involved functional groups, such as –SO_3H, –OH, and the protonated intermediate.

Several descriptors are developed to describe the reactivity of aromatics molecules in electrophilic substitutions. Among these, frontier electron density [$f_r(E)$] derived from Fukui function gives a reasonable description on the soft–soft interactions [32]. $f_r(E)$ represents the density of electrons in the highest occupied molecular orbital (HOMO) [33], where the electrophilic attack prefers to occur at the reaction site with highest electron density. The calculated $f_r(E)$ values for phenol, o-cresol and catechol in organic solvents are given in Table 2. C_4 of Phenol, C_4 of o-cresol and C_4 of catechol are highly reactive for C-alkylations because they hold higher $f_r(E)$. Due to the resonance effect of the nonbonding pz orbitals on the oxygen atoms and the π bonding orbital on the benzene ring, the local charge density and frontier electron density [$f_r(E)$] on oxygen

Table 2
Calculated $f_r(E)$ for phenol, o-cresol in cyclohexane, and catechol in toluene.[a]

Reactant	Solvent	$f_r(E)$		
OH (2) (4)	Cyclohexane	C_2 0.162	C_4 0.303	O 0.386
OH CH₃ (6) (4)	Cyclohexane	C_6 0.127	C_4 0.295	O 0.372
OH OH (3) (4)	Toluene	C_3 0.042	C_4 0.232	O 0.344

[a] $f_r(E)$ on O of catechol is an average value for the two oxygen atoms because they show small difference.

atoms are relatively larger than those on carbon atoms, thus the O-alkylation should be preferred over C-alkylation. Experimental observations show that O-alkylation product TBPE and TBOCE are the main components in the mixture at the beginning of phenol and *o*-cresol tert-butylation, but for catechol, the phenomenon is dramatically different: there is no O-alkylation product TBCE detected throughout the reaction. The different experimental results highlight that apart from the contribution of the HOMO orbital to the reaction path and product selectivity, there should be other factors also impact the reaction kinetics and product selectivity.

3.1. Reaction properties of these tert-butylation reactions

Fig. 1 shows the detailed reaction mechanisms for phenol, *o*-cresol and catechol tert-butylaltion with TBA to form the mono-alkylation products catalyzed by CH_3SO_3H. The three-dimensional structures of each stationary point and transition state, as well as their Cartesian coordinates are provided in Supporting Information Table S2. The energy terms of each structure including electronic energy, ZPE and PCM correction are given in Supporting Information Table S3. The relative stability of the reactants, intermediates, and final products are tabulated in Table 3. By comparison of the relative stability of the reactants and products, the overall reactions for both the C-alkylation and O-alkylation are endothermic. There are differences in the relative stability between the second alkylation intermediates and their deprotonation products. For C-alkylation, the second intermediates are all less stable than the deprotonation products, making formation of C-alkylation products thermodynamically favored. For O-alkylation, the differences in the relative stability between the second O-alkylation intermediates and the deprotonation products vary with the reactants. TBPE is 3.1 kJ/mol more stable than the second intermediate (Int'-O-P). As the ortho-substituent changes to methyl group, the deprotonation product (TBOCE) is 4.6 kJ/mol more stable than the second intermediate (Int'-O-OC), but when it changes to hydroxyl group, the relative stability between TBCE and the second intermediate is reversed, where TBCE is 26.6 kJ/mol less stable than its second intermediate (Int'-O-C), making TBCE formation endothermic. The strong correlation between the ortho-substituent and the relative stability between the second O-alkylation intermediate and deprotonation product is obvious. As the ortho-substituent varies from –H to –CH$_3$, the stability difference between the second O-alkylation intermediate and deprotonation product changes from 3.1 to 4.6 kJ/mol, with the alkylation product more stable. However, when the ortho-substituent changes to –OH, the relative stability between the second O-alkylation intermediate and the alkylation product is reversed, with the intermediate more stable than the product. Therefore, the difference in the relative stability between the second O-alkylation intermediate and alkylation product alters the reaction path and product selectivity.

Apart from the stability of the alkylation intermediate, the product selectivity is also impacted by reaction kinetics, i.e. reaction rate and activation barrier. The energy profiles for each tert-butylation reaction are illustrated in Fig. 2. In phenol tert-butylation, as shown in Fig. 2(a), the activation energy barrier (E_a) for formation of O-alkylation intermediate (Int-O-P) is lowest, which is 105.2 kJ/mol. E_a for formation of C-alkylation intermediates (Int-2-P) and (Int-4-P) are 121.4 and 138.1 kJ/mol, respectively. These E_a values indicate that C-alkylation reactions proceed slower than O-alkylation. For simplification, we did not consider the impact of water adsorption on the subsequent deprotonation steps, thus requiring water desorption prior to deprotonation. The energy difference between the Int and Int' in Fig. 2 results from both the water desorption and $CH_3SO_3^-$ anion transfer. E_a for the subsequent TBPE formation is 28.6 kJ/mol, which is 2.3 and 13.1 kJ/mol lower than that for 2-tert-butyl phenol (2-TBP) and 4-tert-butyl phenol (4-TBP) formation.
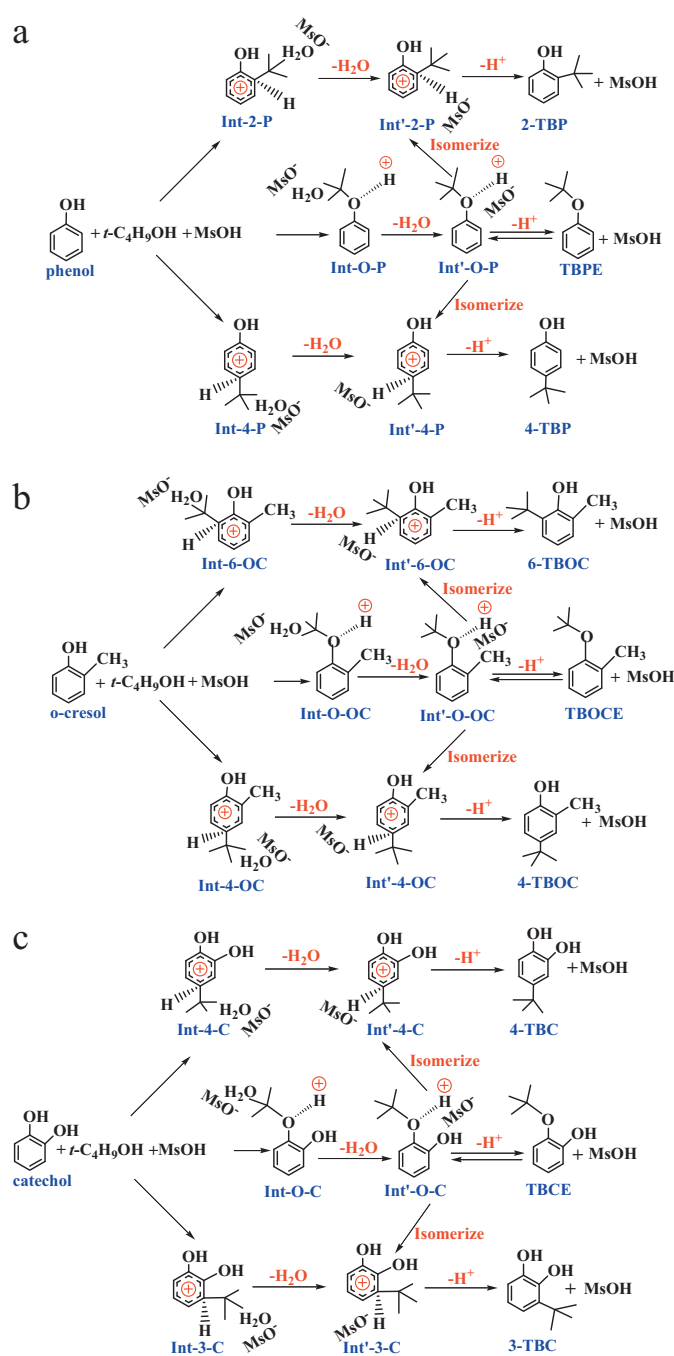

Fig. 1. Proposed reaction paths of (a) phenol tert-butylation in cyclohexane, (b) *o*-cresol tert-butylation in cyclohexane and (c) catechol tert-butylation in toluene. (MsOH represents CH_3SO_3H.)

Therefore, formation of TBPE is faster in the product mixture with high TBA concentration, which explains the high selectivity to TBPE at the beginning in phenol tert-butylation. Some secondary reactions occur to consume TBPE, because there is no TBPE in the final product mixture [13]. TBPE can reverse back to Int'-O-P in this acidic media, which will then isomerize to produce the Int'-2-P or Int'-4-P. The difference in E_a for the forward and reverse reaction of TBPE formation is only 3.1 kJ/mol, so the reaction can be considered equilibrated. The E_a for Int'-O-P isomerization to Int'-2-P is 40.7 kJ/mol, and it is 51.6 kJ/mol for Int'-O-P isomerization to Int'-4-P. The conversion chains from Int'-O-P to other C-alkylation intermediates speed up the consumption of TBPE.

Table 3
Relative energy[a] of each stationary point for phenol, *o*-cresol tert-butylation in cyclohexane, and catechol tert-butylation in toluene.

| Reactant		First intermediate		Second intermediate		Product	
Phenol+		Int-2-P	49.7	Int'-2-P	171.2	2-TBP	110.3
[*t*-C$_4$H$_9$]OH+	0	Int-O-P	31.6	Int'-O-P	160.5	TBPE	157.4
CH$_3$SO$_3$H		Int-4-P	61.2	Int'-4-P	183.7	4-TBP	126.8
o-Cresol+		Int-6-OC	42.0	Int'-6-OC	175.1	6-TBOC	115.4
[*t*-C$_4$H$_9$]OH+	0	Int-O-OC	33.3	Int'-O-OC	150.6	TBOCE	146.0
CH$_3$SO$_3$H		Int-4-OC	42.4	Int'-4-OC	177.9	4-TBOC	121.7
Catechol+		1nt-4-C	53.2	1nt'-4-C	148.3	4-TBC	110.3
[*t*-C$_4$H$_9$]OH+	0	Int-O-C	28.7	Int'-O-C	138.5	TBCE	165.1
CH$_3$SO$_3$H		Int-3-C	70.1	Int'-3-C	195.6	3-TBC	137.7

[a] Energy unit is in kJ/mol.
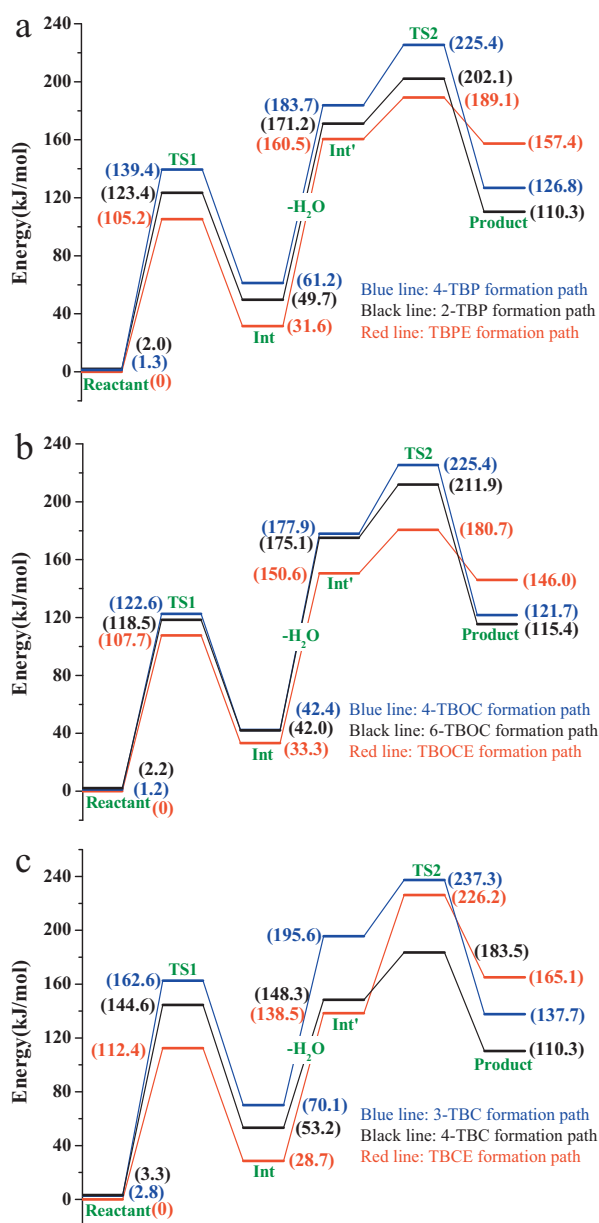
Fig. 2. Energy profiles for (a) phenol tert-butylation in cyclohexane, (b) *o*-cresol tert-butylation in cyclohexane and (c) catechol tert-butylation in toluene. (Energy unit is given in kJ/mol.)

Fig. 2(b) shows that the reaction properties of Brønsted acid-catalyzed tert-butylation of *o*-cresol with TBA are quite similar to that of phenol. E_a for formation of O-alkylation intermediate (Int-O-OC) is lowest, which is 107.7 kJ/mol, and are 116.3 and 121.4 kJ/mol for Int-6-OC and Int-4-OC formation. E_a for *t*-butyl *o*-cresol ether (TBOCE) production is 30.1 kJ/mol, which is 6.7 and 17.4 kJ/mol lower than formation of 6-tert-butyl *o*-cresol (6-TBOC) and 4-tert-butyl *o*-cresol (4-TBOC).

For catechol tert-butylation shown in Fig. 2(c), formation of O-alkylation intermediate (Int-O-C) is faster than C-alkylation intermediate (Int-C-C) formation as well. However, E_a for producing TBCE is 87.7 kJ/mol, which is 52.5 kJ/mol higher than 4-tert-butyl catechol (4-TBC) formation and 46.0 kJ/mol higher than 3-tert-butyl catechol (3-TBC) formation. E_a for the reverse reaction of TBCE formation is 26.6 kJ/mol lower than that for the forward reaction, indicating the fast consumption of TBCE. Moreover, the E_a for isomerization from Int'-O-C to Int'-3-C is 54.7 kJ/mol and is 41.7 kJ/mol to Int'-4-C, which indicate that the isomerization reactions from Int'-O-C to other C-alkylation intermediates are faster compared with TBCE formation from Int'-O-C. Judged from E_a for consuming Int'-O-C, it is more likely to isomerize to Int'-3-C and Int'-4-C rather than producing TBCE.

3.2. Regioselectivity to t-butyl ether

Phenol and *o*-cresol tert-butylation show similar reaction properties, however, the reaction kinetics for catechol tert-butylation is dramatically different, especially for the selectivity to *t*-butyl ether. *t*-Butyl is a large alkyl group, so the steric effect may play an important role in altering the selectivity to *t*-butyl ether, especially for TBCE. Because the C–O bond of the alkylation intermediate may be difficult to be stabilized due to the bulky *t*-butyl group close to an ortho-hydroxyl group. Methyl group is the smallest alkyl group, thus was introduced to compare the steric effect of alkyl group on the regioselectivity to alkyl ether. The relative stability of the transition states (TSs) for formation of alkylation products through deprotonations of the second intermediates with tert-butyl alcohol and methanol as alkylation agents were calculated in cyclohexane solution for phenol and *o*-cresol, but toluene for catechol based on the experimental details [13–15].

Here, we took the most stable TS as the reference point, and the relative stability of other TSs in the same reaction network are compared and given in Table 4. The TSs for both the *t*-butyl phenol ether and methyl phenol ether formation are more stable than other C-alkylation TSs in the same reaction network. For *o*-cresol alkylations, they show the same trend as for phenol. Regarding catechol, the TSs for formation of *t*-butyl catechol ether and methyl catechol ether are both less stable than those for 4-alkylation product formation, but more stable than those for 3-alkylation product formation. The above computational results indicate that the relative stability rules of the transition states for alkyl ether product formation

Table 4
Relative energy[a] of each transition state for the deprotonation step to form the alkylation product using t-C_4H_9OH and CH_3OH as the electrophilic agents.[b]

Reactant	Relative energy of the TS for the deprotonation step using t-C_4H_9OH			Relative energy of the TS for the deprotonation step using CH_3OH		
Phenol	TS(O-) 0	TS(4-) 36.3	TS(2-) 13.0	TS(O-) 0	TS(4-) 27.3	TS(2-) 9.1
o-Cresol	TS(O-) 0	TS(4-) 44.7	TS(6-) 31.2	TS(O-) 0	TS(4-) 33.7	TS(6-) 28.9
Catechol	TS(O-) 42.7	TS(4-) 0	TS(3-) 53.8	TS(O-) 31.5	TS(4-) 0	TS(3-) 52.7

[a] Energy unit is in kJ/mol.
[b] TS(O-) represents the transition state for producing ether product, others represent the transition states for producing C-alkylation products.
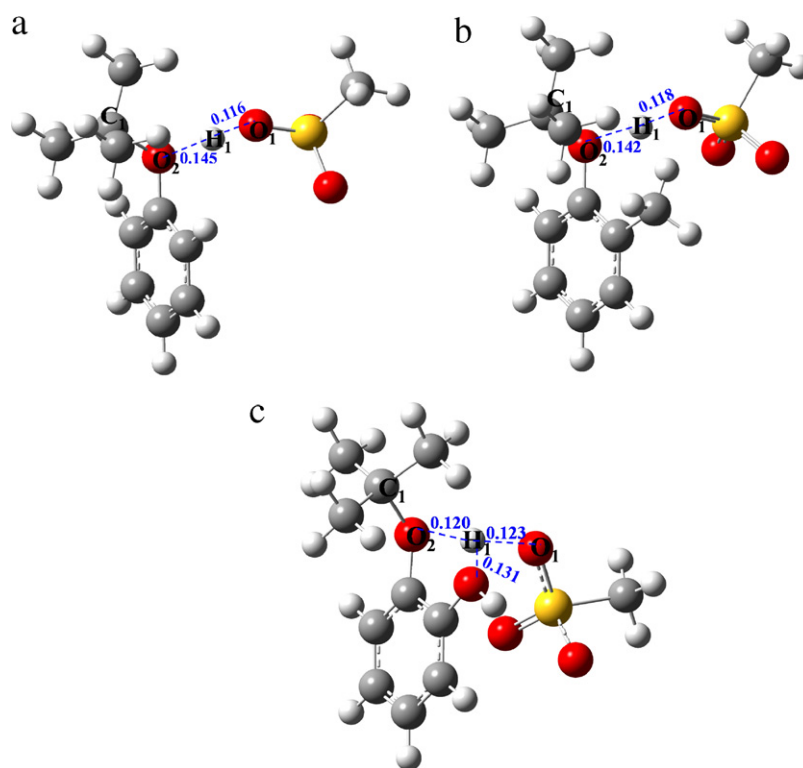
Fig. 3. Optimized geometries of the transition states for formation of (a) TBPE, (b) TBOCE and (c) TBCE.

do not change with the electrophilic substituted agent vary from a bulky t-butyl group to a smaller methyl group, which proves that the steric effect of t-butyl group does not have a significant impact on the regioselectivity to t-butyl ether.

However, there are dramatic differences in TS relative stability order and the E_a for formation of TBPE, TBOCE and TBCE. Therefore, we examined the corresponding molecular structures of the TSs for deprotonation steps within these three tert-butylation reactions. The optimized TS geometries for formation of TBPE (a), TBOCE (b) and TBCE (c) are shown in Fig. 3, and relevant geometric parameters of the three TSs are given in Table 5. From Fig. 3, it is apparent that the TS configurations involve the trend of proton transfer from the protonated intermediate to the $CH_3SO_3{}^-$ anion. The original O_2–H_1 bond cleavage in the TS is observed through the elongation of the bond length. The O_2–H_1 bond length elongates to 0.145 from 0.098 nm in the second alkylation intermediate for phenol, 0.142 from 0.097 nm for o-cresol, and 0.120 from 0.097 nm for catechol. The O_1–H_1 distance becomes smaller, which contracts to 0.116 nm for phenol, 0.118 nm for o-cresol and 0.123 nm for catechol. The O_2–H_1 distance is smaller, but the O_1–H_1 distance is longer in TS (c) compared with TS (a) and TS (b). In particular, within TS(c), there is an additional intramolecular hydrogen bond (IMHB)

formed between the proton and the ortho-hydroxyl group with the O–H distance of 0.131 nm, as shown in Fig. 3(c). Despite the anion of CH_3SO_3H exhibits superior proton affinity than phenol-hydroxyl group, the above results indicate that the proton would rather bind with the hydroxyl group within Int'-O-C than interact with the anion of CH_3SO_3H.

In order to clarify the impact of IMHB on the selectivity to TBCE, we fall back to the structures and energies of catechol, its protonated intermediate and the deprotonation transition state, as shown in Fig. 4. There are two hydroxyl groups within a catechol molecule seen from Fig. 4(b), and they should form an IMHB to gain extra stability of 11.4 kJ/mol compared with structure (a). The for-

Table 5
Optimized geometric parameters of the transition states for formation of TBPE [TS(a)], TBOCE [TS(b)] and TBCE [TS(c)].

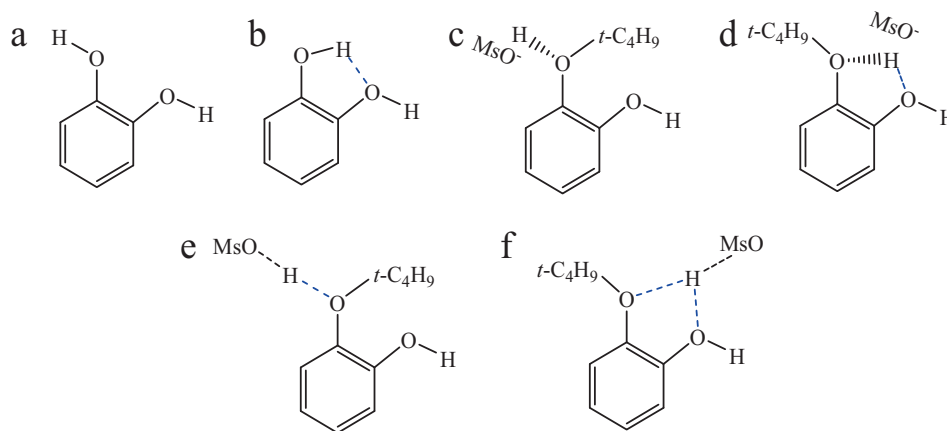| Parameter	TS(a)	TS(b)	TS(c)
O_2–H_1 (nm)	0.145	0.142	0.120
O_1–H_1 (nm)	0.116	0.118	0.123
C_1–O_2 (nm)	0.160	0.159	0.154
H_1–O_2–C_1 (°)	109.5	111.3	108.9

Fig. 4. Intramolecular hydrogen bond formed within (b) catechol molecule, (d) its protonated intermediate and (f) transition state for deprotonation step; structure (a), (c) and (e) are used for comparison. (MsOH represents CH_3SO_3H.)

mation barrier of this IMHB is 11.9 kJ/mol, which is very modest. So, the IMHB must exist within a catechol molecule. For Int'-O-C shown in Fig. 4(d), an IMHB still exists, between the ortho-hydroxyl group and the proton. The formation barrier of this IMHB is 12.0 kJ/mol, and can result in extra stability of 20.1 kJ/mol compared with structure (c). With formation of an IMHB, the proton affinity of the intermediate is further altered. The protonation energy of TBCE is 88.1 kJ/mol higher than that of catechol, which indicates that formation of the IMHB can stabilize the TBCE in its protonated form (Int'-O-C). Formation of TBCE goes through deprotonation of the protonated intermediate. Within the structure of the deprotonation transition state shown in Fig. 4(f), there is still an additional IMHB formed between the proton and ortho-hydroxyl group, which inhibits the proton transfer from the protonated intermediate to $CH_3SO_3^-$ anion, as reflected by the bond parameters given in Fig. 3 (c). Formation of the IMHB makes the protonated intermediate more stable, and increases the E_a for deprotonation step to produce TBCE. The isomerization barriers from Int'-O-C to Int'-3-C (54.7 kJ/mol) and Int'-4-C (41.7 kJ/mol) are also lower than E_a for producing TBCE (87.7 kJ/mol). Therefore, the formed Int'-O-C will be consumed fast by the isomerization reactions instead of producing TBCE.

4. Conclusions

The reaction mechanisms of Brønsted acid-catalyzed tert-butylation of phenol, o-cresol and catechol have been examined by a comparative computational study. The steric effect of t-butyl group does not have an apparent impact on the regioselectivity to t-butyl ether. The differences in the stability of O-alkylation intermediates, resulted from different ortho-substituents of the reactants, account for the regioselectivity to t-butyl ether. The intramolecular hydrogen bond formed within O-alkylation intermediate facilitates its isomerization to C-alkylation intermediates, inhibits the t-butyl catechol ether formation, thus making the reaction kinetics for catechol tert-butylation unique.

Acknowledgements

Appendix A. Supplementary data

Supplementary data associated with this article can be found, in the online version, at doi:10.1016/j.molcata.2010.09.010.

References

[1] D.W. Park, N.Y. Mun, K.H. Kim, I. Kim, S.W. Park, Catal. Today 115 (2006) 130–133.
[2] C. Lansalot-Matras, C. Moreau, Catal. Commun. 4 (2003) 517–520.
[3] H.B. Zhao, J.E. Holladay, H. Brown, Z.C. Zhang, Science 316 (2007) 1597–1600.
[4] L.Y. Piao, X. Fu, Y.L. Yang, G.H. Tao, Y. Kou, Catal. Today 93–95 (2004) 301–305.
[5] T. Welton, Chem. Rev. 99 (1999) 2071–2084.
[6] S. Chowdhury, R.S. Mohan, J.L. Scott, Tetrahedron 63 (2007) 2363–2389.
[7] P. Wasserscheid, W. Keim, Angew. Chem. Int. Ed. 39 (2000) 3773–3789.
[8] R. Sheldon, Chem. Commun. (2001) 2399–2407.
[9] H.Y. Shen, Z.M.A. Judeh, C.B. Ching, Tetrahedron Lett. 44 (2003) 981–983.
[10] S.W. Liu, C.X. Xie, S.T. Yu, F.S. Liu, K.H. Ji, Catal. Commun. 9 (2008) 1634–1638.
[11] J.Z. Gui, H.Y. Ban, X.H. Cong, X.T. Zhang, Z.D. Hu, Z.L. Sun, J. Mol. Catal. A: Chem. 225 (2005) 27–30.
[12] K. Kondamudi, P. Elavarasan, P.J. Dyson, S. Upadhyayula, J. Mol. Catal. A: Chem. 1–2 (2010) 34–41.
[13] X.M. Liu, X.W. Guo, M. Liu, Petrolei Sinica (Petroleum Processing Section) 24 (2008) 216–221.
[14] L. Gao, M. Liu, X.W. Nie, X.W. Guo, Petrolei Sinica (Petroleum Processing Section) 1 (2010) 115–121.
[15] X.W. Nie, X. Liu, L. Gao, M. Liu, C.S. Song, X.W. Guo, Ind. Eng. Chem. Res 49 (2010) 8157–8163.
[16] X.M. Liu, J.X. Zhou, X.W. Guo, M. Liu, X.L. Ma, C.S. Song, C. Wang, Ind. Eng. Chem. Res. 47 (2008) 5298–5303.
[17] X.M. Liu, M. Liu, X.W. Guo, J.X. Zhou, Catal. Commun. 9 (2008) 1–7.
[18] J.W. Yoo, C.W. Lee, S.E. Park, J.J. Ko, Appl. Catal. A 187 (1999) 225–232.
[19] C.H. Zhou, Z.H. Ge, X.N. Li, D.S. Tong, Q.W. Li, H.Q. Guo, Chin. J. Chem. Eng. 12 (2004) 388–394.
[20] M.J. Frisch, G.W. Trucks, H.B. Schlegel, G.E. Scuseria, M.A. Robb, J.R. Cheeseman, J.A. Montgomery, J.T. Vreven, K.N. Kudin, J.C. Burant, J.M. Millam, S.S. Iyengar, J. Tomasi, V. Barone, B. Mennucci, M. Cossi, G. Scalmani, N. Rega, G.A. Petersson, H. Nakatsuji, M. Hada, M. Ehara, K. Toyota, R. Fukuda, J. Hasegawa, M. Ishida, T. Nakajima, Y. Honda, O. Kitao, H. Nakai, M. Klene, X. Li, J.E. Knox, H.P. Hratchian, J.B. Cross, C. Adamo, J. Jaramillo, R. Gomperts, R.E. Stratmann, O. Yazyev, A.J. Austin, R. Cammi, C. Pomelli, J.W. Ochterski, P.Y. Ayala, K. Morokuma, G.A. Voth, P. Salvador, J.J. Dannenberg, V.G. Zakrzewski, S. Dapprich, A.D. Daniels, M.C. Strain, O. Farkas, D.K. Malick, A.D. Rabuck, K. Raghavachari, J.B. Foresman, J.V. Ortiz, Q. Cui, A.G. Baboul, S. Clifford, J. Cioslowski, B.B. Stefanov, G. Liu, A. Liashenko, P. Piskorz, I. Komaromi, R.L. Martin, D.J. Fox, T. Keith, M.A. Al-Laham, C.Y. Peng, A. Nanayakkara, M. Challacombe, P.M.W. Gill, B. Johnson, W. Chen, M.W. Wong, C. Gonzalez, J.A. Pople, Gaussian 03 (Revision E.01), Gaussian, Inc., Pittsburgh, PA, 2003.
[21] B. Miehlich, A. Savin, H. Stoll, H. Preuss, Chem. Phys. Lett. 157 (1989) 200–206.
[22] A.D. Becke, J. Chem. Phys. 98 (1993) 5648–5652.
[23] C.T. Lee, W.T. Yang, R.G. Parr, Phys. Rev. B 37 (1988) 785–789.
[24] A.D. McLean, G.S. Chandler, J. Chem. Phys. 72 (1980) 5639–5648.
[25] C. Gonzalez, H.B. Schlegel, J. Chem. Phys. 90 (1989) 2154–2161.
[26] C. Gonzalez, H.B. Schlegel, J. Phys. Chem. 94 (1990) 5523–5527.
[27] E. Cances, B. Mennucci, J. Tomasi, J. Chem. Phys. 107 (1997) 3032–3041.

[28] B. Mennucci, J. Tomasi, J. Chem. Phys. 106 (1997) 5151–5158.
[29] M. Cossi, G. Scalmani, N. Rega, V. Barone, J. Chem. Phys. 117 (2002) 43–54.
[30] M. Cossi, V. Barone, B. Mennucci, J. Tomasi, Chem. Phys. Lett. 286 (1998) 253–260.
[31] T. Harris, C. Campbell, Y.C. Tang, J. Phys. Chem. A 110 (2006) 2246–2252.
[32] W. Langenaeker, K. Demel, P. Geerlings, J. Mol. Struct. Theochem. 234 (1991) 329–342.
[33] C. Song, X. Ma, A.D. Schmitz, H.H. Schobert, Appl. Catal. A 182 (1999) 175–181.